



## Analysis on Band Layer Design and J-V characteristics of Zinc Oxide Based Junction Field Effect Transistor

Ms Chaw Su Nandar Hlaing<sup>1</sup>, Thiri Nwe<sup>1</sup>

<sup>1</sup> Department of Electronic Engineering, Technological University (Mandalay), Mandalay, Myanmar



\*Corresponding Author: Chaw Su Nandar Hlaing

### Article Info

#### Article history:

Received 11 June 2020

Received in revised form 17 June 2020

Accepted 20 June 2020

#### Keywords:

JFET

ZnO

Numerical Analysis

Band Gap Energy

MATLAB

### Abstract

This paper presents the band gap design and J-V characteristic curve of Zinc Oxide (ZnO) based on Junction Field Effect Transistor (JFET). The physical properties for analysis of semiconductor field effect transistor play a vital role in semiconductor measurements to obtain the high-performance devices. The main objective of this research is to design and analyse the band diagram design of semiconductor materials which are used for high performance junction field effect transistor. In this paper, the fundamental theory of semiconductors, the electrical properties analysis and bandgap design of materials for junction field effect transistor are described. Firstly, the energy bandgaps are performed based on the existing mathematical equations and the required parameters depending on the specified semiconductor material. Secondly, the J-V characteristic curves of semiconductor material are discussed in this paper. In order to achieve the current-voltage characteristic for specific junction field effect transistor, numerical values of each parameter which are included in analysis are defined and then these resultant values are predicted for the performance of junction field effect transistors. The computerized analyses have also mentioned in this paper.

### Introduction

The technology of junction field effect transistor (JFET) based on zinc oxide (ZnO) channel layer has undergone a rapid development in recent years. The use of ZnO channel layer for IC circuits offers some outstanding advantages over the traditional Si channel layer, especially in the area of high frequency and high-speed microwave circuits. Its application extends to low noise preamplifiers and linear amplifiers, oscillators and mixers in communication networks due to some of its outstanding physical properties, such as high cut-off frequency (more than 10GHz for 1 $\mu$ m gate length) and high electron mobility. Furthermore, ZnO circuits are suited of optoelectronic applications due to its direct bandgap property which can be grown with semi-insulating bulk conductivity. At the same time, the commercial availability of improved technology, such as, dry etching, plasma-enhanced chemical vapor deposition, sub-micro meter optical lithography, and rapid thermal annealing equipment have made the fabrication for advanced ZnO JFETs simpler and lower cost (Sze, 2008; Neamen, 2012; Li, 2012).

The proposed structure of ZnO JFET has been developed by using ZnO material for channel layer. At first, the specific substrate of sapphire material was used and the ZnO layer could be

deposited upon the substrate for channel layer. After that gate electrode ( $\text{SiO}_2$ ) has been developed by using pulse laser deposition (PLD) techniques. Figure 1.1 shows the proposed structure of JFET for this works.

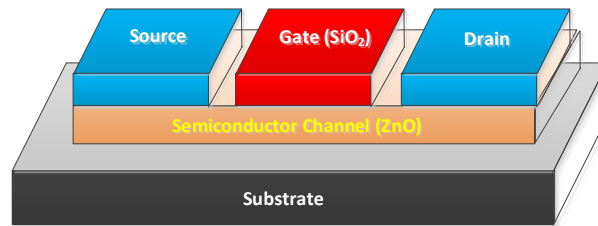


Figure 1.1 Proposed Structure of the ZnO JFET system

The rest of the paper is catalogued as follows. Section II describes the theoretical background of ZnO based JFET. Section III mentions the energy band gap, current density and voltage characteristic curve with appropriate formula. Section IV discusses on the results of the implementation. After all section V concludes the research work.

### Background Theory

This section describes the theoretical background for zinc oxide (ZnO) semiconductor material and junction field effect transistor (JFET).

#### Zinc Oxide Material as A Semiconductor Material

ZnO is a wide-band gap semiconductor of the II-VI semiconductor group. ZnO has a relatively large direct band gap of  $\sim 3.37$  eV at room temperature. This wide band gap has many advantages like higher breakdown voltage, ability to sustain large electrical fields, lower electronic noise, high temperature and high-power operation. These properties make ZnO nanomaterial fit for wide varieties of electrical applications. They are high exciton binding energy, ability to grow high quality single crystal substrate with low cost and simple crystal growth technology. Electron mobility of ZnO strongly dependent on temperature and possess a maximum of  $\sim 2000$   $\text{cm}^2/(\text{V}\cdot\text{s})$  at 80 K.

It can be afforded superior hardness compared with other semiconductor materials, such as Si, GaAs, CdS, and GaN. Figure 1.2 shows the two main forms of zinc oxide (ZnO) material. They are hexagonal wurtzite & cubic zinc blende crystal structure. The wurtzite structure is most stable at ambient conditions and thus most common. The zincblende form can be stabilized by growing ZnO on substrates with cubic lattice structure (Feng, 2013).

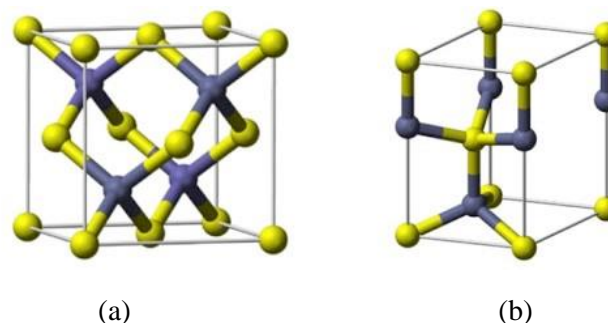


Figure 1.2 Two types of Crystal Structure for zinc oxide (ZnO) material (a) wurtzite & cubic zinc blende crystal structure (Feng, 2013)

## Junction Field Effect Transistor

Junction field effect transistor is the simplest type of field effect transistor. This is the three-terminal semiconductor device that can be electronically used as controlled switches, amplifiers, or voltage-controlled resistors. The semiconductor material in a JFET is positively and negatively doped and arranged to form a channel for effective functioning of the device. In a JFET, the semiconductor doped with donor impurities forms an n-type channel, whereas a semiconductor doped with acceptor impurities forms a p-type region (Sze, 2008).

An electrical connection at the end of the channel on a JFET is either a drain terminal or source terminal, and the middle terminal is known as a gate. These terminals are actually p-n junctions with the main channel. The source terminal (S) is the terminal through which the majority carriers enter the channel. The terminal, through which the majority carriers leave the channel, is called the drain terminal (D). In the gate terminal (G), there are two internally connected heavily doped impurity regions formed by alloying, by diffusion, or by any other method available to create two P-N junctions. The region between the source and drain, sandwiched between the two gates is called the channel and the majority carriers move from source to drain through this channel. Figure 1.3 demonstrates the basic structure of n-channel junction field effect transistor (JFET) (Li, 2012).

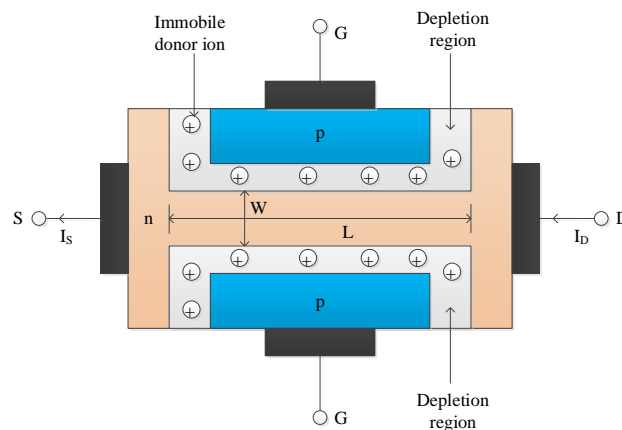


Figure 1.3 Basic Structure of N-channel Junction Field Effect Transistor

## Band Diagram Condition and Characteristic Analysis

In this section, energy band diagram of ZnO heterojunction material and its properties are reported. Mathematical explanations are briefly described and test results of the design structure are shown. The equilibrium condition of p-n junction design, the electron and hole concentration of zinc oxide material and J-V characteristic curve are described in this section.

### Band Structure of n-ZnO and p-SiO<sub>2</sub> Heterojunction

In the band diagram design of n-ZnO/p-SiO<sub>2</sub> heterojunction,  $N_A=1 \times 10^{16} \text{ cm}^{-3}$  and  $N_d=1 \times 10^{17} \text{ cm}^{-3}$  are used as doping concentration for P-region and n-region. Under thermal equilibrium conditions (i.e. no biasing voltage), when the two materials are joining, the Fermi level will be a constant line across the junction. These materials have different band gap but typically have different doping (Singleton, 2001).

Table 1.1 Required Input Parameters of ZnO and SiO<sub>2</sub> Materials (Berger, 1996)

Required Input Parameters	ZnO	SiO <sub>2</sub>

Band-gap energy, $E_g$ (eV)	3.37	8.9
Permittivity, $\epsilon_r$	8.5	3.9
Electron affinity, $\chi$	4.1	0.95

Different doping level was happened band banding and depletion region was formed. Although the process of heterojunction structure is similar to that of homojunction structure, there are band edge discontinuities in homojunction. This is the fundamental concepts for fabricating the JFET design. For energy band analysis of the research work, the energy band-gap of zinc oxide (ZnO) and silicon dioxide (SiO<sub>2</sub>) are 3.37 eV and 8.9eV (Purbayanto et al, 2019). And the intrinsic carrier concentration of zinc oxide (ZnO) and silicon dioxide (SiO<sub>2</sub>) are  $2.807 \times 10^{-10} \text{ cm}^{-3}$  and  $1.075 \times 10^{-56} \text{ cm}^{-3}$ , respectively [4-7]. The required parameters of zinc oxide (ZnO) and silicon dioxide (SiO<sub>2</sub>) are shown in Table 1.1 (Berger, 1996).

Based on the Anderson model, the conduction and valence band offsets ( $\Delta E_c$  and  $\Delta E_v$ ) from the energy band diagram are given by:

$$\Delta E_c = q(\chi_1 - \chi_2) \quad (1)$$

$$\Delta E_v = (E_{g\text{SiO}_2} - E_{g\text{ZnO}}) - \Delta E_c = \Delta E_g - \Delta E_c \quad (2)$$

The electrostatic potentials ( $\phi_n$  and  $\phi_p$ ) at the depletion layer edge of the n-region and p-region and the built-in potential of a p-n junction are defined by,

$$\phi_n = V_T \ln \frac{N_d}{n_i} \quad (3)$$

$$\phi_p = -V_T \ln \frac{N_A}{n_i} \quad (4)$$

The built-in potential of a p-n junction are described by,

$$V_{bi} = \phi_n - \phi_p = V_T \ln \frac{N_d N_A}{n_i^2} \quad (5)$$

Using the depletion approximation,  $V_{b\text{ZnO}}$  and  $V_{b\text{SiO}_2}$  in the n-ZnO and P-SiO<sub>2</sub> regions can be expressed by,

$$V_{b\text{SiO}_2} = V_{bip} = \frac{\epsilon_{\text{ZnO}} \epsilon_0 N_d}{\epsilon_{\text{ZnO}} \epsilon_0 N_d + \epsilon_{\text{SiO}_2} \epsilon_0 N_A} V_{bi} \quad (6)$$

$$V_{b\text{ZnO}} = V_{bin} = \frac{\epsilon_{\text{SiO}_2} \epsilon_0 N_A}{\epsilon_{\text{ZnO}} \epsilon_0 N_d + \epsilon_{\text{SiO}_2} \epsilon_0 N_A} V_{bi} \quad (7)$$

Under thermal equilibrium condition, the depletion layer widths on either side of the n-ZnO and P-SiO<sub>2</sub> heterojunction are given by Singleton (2001):

$$x_n = \left[ \left( \frac{2\epsilon_{\text{ZnO}} \epsilon_0 V_{bi}}{q} \right) \left( \frac{N_d + N_A}{N_d} \right) \right]^{1/2} \quad (8)$$

$$x_p = \left[ \left( \frac{2\varepsilon_{\text{SiO}_2} \varepsilon_0 V_{bi}}{q} \right) \left( \frac{N_d + N_A}{N_A} \right) \right]^{1/2} \quad (9)$$

where  $\chi_1$  is the electron affinity for zinc oxide material and  $\chi_2$  is the electron affinity for silicon dioxide material,  $V_{b\text{SiO}_2}$  and  $V_{b\text{ZnO}}$  are built-in potentials for silicon dioxide material and zinc oxide material,  $\varepsilon_{\text{ZnO}}$  and  $\varepsilon_{\text{SiO}_2}$  are permittivities for zinc oxide material and silicon dioxide material and  $N_d$  is the donor concentration for zinc oxide material and  $N_A$  is the acceptor concentration for silicon dioxide material (Singleton, 2001; Su et al, 2014).

### J-V Characteristic Curve for p-type gate SiO<sub>2</sub> and n-channel ZnO JFET

The acceptor concentration and donor concentration are  $N_A = 1 \times 10^{16} \text{ cm}^{-3}$  and  $N_d = 1 \times 10^{17} \text{ cm}^{-3}$ . The intrinsic carrier concentration for ZnO and SiO<sub>2</sub> are the following:

$$n_i = (N_C N_V)^{1/2} \exp\left(-\frac{E_g}{2kT}\right) = 3.393 \times 10^{-10} \text{ cm}^{-3} \quad \text{and} \quad n_i = (N_C N_V)^{1/2} \exp\left(-\frac{E_g}{2kT}\right) = 1.075 \times 10^{-56} \text{ cm}^{-3}.$$

The minority carriers mobilities for P-type and n-type of these materials are  $\mu_n = 200 \text{ cm}^2/\text{V.s}$  and  $\mu_p = 4500 \text{ cm}^2/\text{V.s}$  (Berger, 1996; Sze, 2008; Neamen, 2012; Li, 2012).

The diffusion coefficients are:

$$D_n = \frac{kT\mu_n}{e} = (0.02585\text{V})(200\text{cm}^2\text{V}^{-1}\text{s}^{-1}) = 5.175\text{cm}^2\text{s}^{-1}$$

$$D_p = \frac{kT\mu_p}{e} = (0.02585\text{V})(4500\text{cm}^2\text{V}^{-1}\text{s}^{-1}) = 116.325\text{cm}^2\text{s}^{-1}.$$

The radiative recombination is the unavoidable recombination and the radiative lifetime is associated to the radiative coefficient of material. The minority carrier lifetimes or radiative lifetimes of carriers are (Neamen, 2012):

$$\tau_n = \frac{\mu_n m_e^*}{e} = \frac{(200 \times 10^{-4} \text{ m}^2 \text{ V}^{-1} \text{ s}^{-1}) \times (0.28 \times 9.1 \times 10^{-31} \text{ kg})}{1.6 \times 10^{-19} \text{ C}} = 3.1885 \times 10^{-14} \text{ s}$$

$$\tau_p = \frac{\mu_p m_h^*}{e} = \frac{(4500 \times 10^{-4} \text{ m}^2 \text{ V}^{-1} \text{ s}^{-1}) \times (0.58 \times 9.1 \times 10^{-31} \text{ kg})}{1.6 \times 10^{-19} \text{ C}} = 1.484 \times 10^{-12} \text{ s}$$

The diffusion lengths of the minority carriers are:

$$L_n = \sqrt{D_n \tau_n} = \sqrt{(5.175 \text{ cm}^2 \text{ s}^{-1}) \times (3.1885 \times 10^{-14} \text{ s})} = 4.062 \times 10^{-7} \text{ cm}$$

$$L_p = \sqrt{D_p \tau_p} = \sqrt{(116.325 \text{ cm}^2 \text{ s}^{-1}) \times (1.484 \times 10^{-12} \text{ s})} = 1.314 \times 10^{-5} \text{ cm}$$

The total current density is described by the following:

$$J = \left( \frac{eD_p}{L_p N_d} + \frac{eD_n}{L_n N_A} \right) n_i^2 \left[ \exp\left(\frac{eV}{kT} - 1\right) \right] \quad (10)$$

where;  $m_e^*$  = electron effective mass,  $0.28m_0$

$m_h^*$  = hole effective mass,  $0.58m_0$

$m_0$  = rest mass of electron and hole,  $9.1 \times 10^{-31} \text{ kg}$

- e = electric charge,  $1.6 \times 10^{-19}$  C
- k = Boltzmann's constant,  $1.38 \times 10^{-23}$  J/K
- T = temperature, 300K
- V = forward voltage [2]

## Results and Discussion

This section includes results and discussion on band diagram condition and J-V characteristics of the ZnO-based JFET.

To improve the band layer analysis, the hole and electron concentrations are important parameters. The hole concentration depends on the doping concentration of the material. Figure 1.4 shows a plot of minority carrier concentration, hole for n-channel zinc oxide material as a function of doping concentration. According to the result, hole concentration is decreased when the doping concentration is increased.

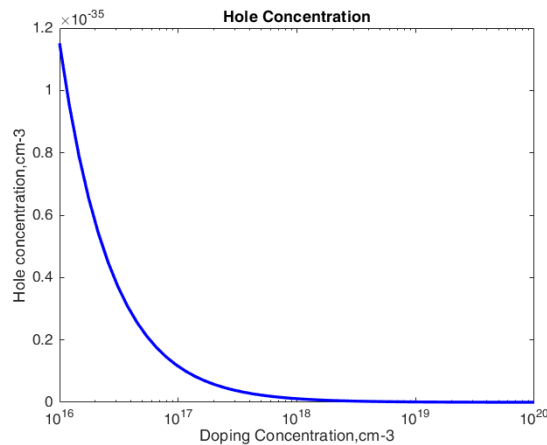


Figure 1.4 Hole Concentration as a Function of Doping Concentration

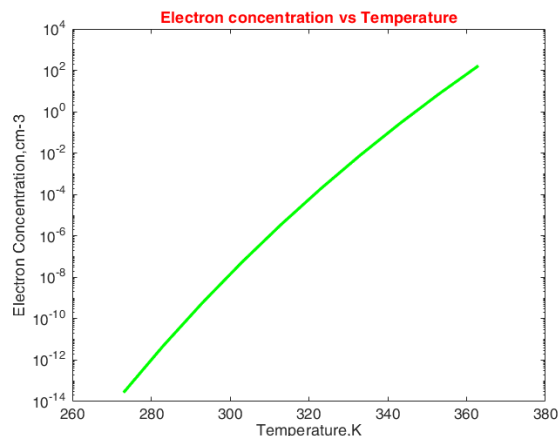


Figure 1.5 Electron Concentration Depending on Temperature

Figure 1.5 illustrates the majority carrier concentration, electron for ZnO material depending on the temperature. It should be noted that the majority carrier concentrations, electron is greater than the minority carrier concentrations, hole. As the temperature is increased, the electron concentration also increases.

The band structure of an unbiased n-ZnO/P-SiO<sub>2</sub> heterojunction is shown in Figure 1.6. The figure shows that the position of P-type semiconductor is larger than the n-type semiconductor. As a result, the total width of the depletion region is 0.131  $\mu\text{m}$ . The band edge discontinuities for conduction band is 93.484 meV and for valence band is 181.187 meV. The conduction band is closer to the Fermi level than the valence band.

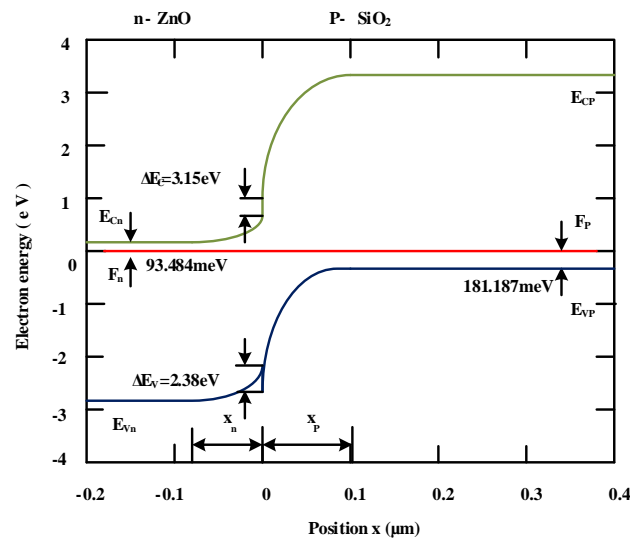


Figure 1.6 Heterojunction Band Structure of n-ZnO/P-SiO<sub>2</sub>

The conduction band edge for P-type is obtained from the difference in the energy gap and the fermi level of the P-type material. Then, the band decreases according to the potential drop and finally close to the fermi level. A similar configuration can occur for valence band. From the design of the band diagram, the conditions of the drift current or diffusion current flowing across the heterojunction can be observed.

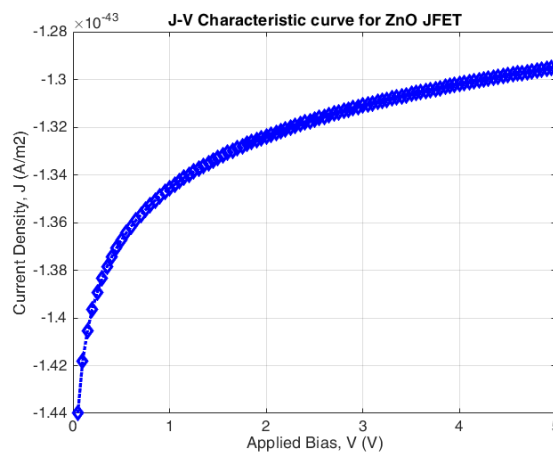


Figure 1.7 J-V Characteristic Curve for JFET using ZnO Material

Figure 1.7 demonstrates the resultant characteristic curve of current density and applied bias using zinc oxide (ZnO) semiconductor material for junction field effect transistor. When the applied bias is increased, the total current density is also increased.

## Conclusion

The paper has been to describe the band layer design and J-V characteristics of high-performance of junction field effect transistor. The pn junction band structure are calculated and designed as bands that can be used for high performance zinc oxide-based junction field effect transistor. The parameters are used for zinc oxide material and it is confirmed that the characteristic curves for transistor design will increase the performance of the device to be used in the real world. The development of the device with the help of computerized analysis will be provided the better characteristics and performance of JFET.

## Acknowledgment

The author would like to acknowledge many colleagues from the semiconductor research group under the Department of Electronic Engineering of Technological University (Mandalay). This work has been supported by our parents to complete for the requirements of degree program at TUM.

## References

- Berger, L. I. (1996). *Semiconductor materials*. CRC press.
- Feng, Z. C. (Ed.). (2013). *Handbook of Zinc Oxide and Related Materials: Devices and Nano-engineering. Volume Two*. CRC Press/Taylor & Francis.
- Li, S. S. (2012). *Semiconductor physical electronics*. Springer Science & Business Media.
- Neamen, D. A. (2012). *Semiconductor physics and devices: basic principles*. New York, NY: McGraw-Hill.
- Purbayanto, M. A. K., Ichwan, R., Nurfani, E., & Darma, Y. (2019). Critical point analysis of dielectric constant in ZnO thin films on different electronic environments. In *Journal of Physics: Conference Series* (Vol. 1204, No. 1, p. 012118). IOP Publishing.
- Singleton, J. (2001). *Band theory and electronic properties of solids* (Vol. 2). Oxford University Press.
- Su, L., Zhang, Q., Wu, T., Chen, M., Su, Y., Zhu, Y., ... & Tang, Z. (2014). High-performance zero-bias ultraviolet photodetector based on p-GaN/n-ZnO heterojunction. *Applied Physics Letters*, 105(7), 072106.
- Sze, S. M. (2008). *Semiconductor devices: physics and technology*. John wiley & sons.